Arch. Metall. Mater. **71** (2026), 3, 793-805

DOI: https://doi.org/10.24425/amm.2026.1970

JERZY JEDLIŃSKI[1*], HYUN-JU CHOI[2#], YONGHO SOHN[2]

SCALE EVOLUTION DURING EARLY OXIDATION STAGES OF POLYCRYSTALLINE β-NiAl AT 1100°C AND THE EFFECT OF IMPLANTED YTTRIUM

The development of scales at early oxidation stages was studied in terms of the evolution of their morphology and phase composition on unmodified and Yttrium-implanted β-NiAl intermetallic compound at 1100°C in air for exposure periods from 3 min up to 24 hours and Scanning Electron Microscopy, Low-Angle X-ray Diffraction and Photoluminescence Spectroscopy. Similar consecutive stages of the scale evolution were found on both materials and implanted yttrium retarded the rate of this process which manifested itself mainly in impeding the phase transformation of transient aluminium oxides into α-Al_2O_3, the required protective layer. The scale evolution had a local nature and under the same oxidation conditions the regions sometimes co-existed, exhibiting different stages of the evolution. No unambiguous relationship was found between the scale morphology and its phase composition.

Keywords: β-NiAl; Yttrium-effect; Alumina scale

1. Introduction

Beta (β) NiAl (B2) is well-known material applied as a bond coat in thermal barrier coating (TBC) systems to protect the underlying Ni-based superalloys against degradation caused by high temperature oxidation ($T > \sim 1000°C$). Its substantial oxidation resistance provided through the formation of protective α-Al_2O_3 scale has been known for a long time and studied for almost 50 years, as evidenced by the first reported results (eg. [1-4]) An outstanding improvement in performance of the β-NiAl (and other alumina formers) brought about by small amounts (of order of 0.1 wt.% or even less) of reactive elements (e.g. Y, Hf, Zr) and/or higher amounts of noble metals, mainly Pt, has been observed, which results in the presence of additions of these elements in this materials as well as in other alumina formers, structural and coatings, applied in oxidizing atmospheres. However, despite a vast evidence of experimental data obtained over last few decades, e.g. [5-19] for β-NiAl, the reasons for this beneficial effect, usually referred to as the reactive-element effect (REE), cannot yet be considered fully explained. Intensive research has not only allowed for significant progress in understanding REE, which has been successively reported [20-27], but also indicated that the complexity of the processes occurring during oxidation requires an updated approach that combines the use of modern research methods and advanced modelling of processes occurring in the entire reacting system, including specific regions, in particular interfacial ones. The first effects of this approach have already led to going beyond the previously proposed concept of dynamic-segregation theory [28], although without negating it [29-31].

It should be emphasized that the experimental procedure ought to be adapted to meet specific needs, which depend largely on the type of material being studied. It relies on the appropriate planning the oxidation exposure conditions. In the case of scales growing on β-NiAl their characteristic feature is relatively slow and having local nature evolution. The former is manifested by the relatively prolonged stability of undesirable transition aluminium oxides compositions (γ-, δ-, θ-Al_2O_3), while the latter by development and subsequent co-existence during the transient oxidation stages of several features (blade-like grains, patches, ridges, and cracks).

Thus, a pertinent question arises, whether and what impact these features have on the protective properties of the stable alumina protective scales and long-term resistance to oxidation of the material. Addressing this problem requires exploring in detail the process of α-Al_2O_3 protective scale formation, i.e. investigating its consecutive stages.

[1] AGH UNIVERSITY OF KRAKOW, FACULTY OF MATERIALS SCIENCE AND CERAMICS, AL. A. MICKIEWICZA 30, 30-059 KRAKOW, POLAND
[2] UNIVERSITY OF CENTRAL FLORIDA, ADVANCED MATERIALS PROCESSING AND ANALYSIS CENTER AND DEPARTMENT OF MECHANICAL, MATERIALS AND AEROSPACE ENGINEERING, ORLANDO, FL 32816. USA

[#] Currently: Korean Automotive Technology Institute, Cheonan, 31214 Republic of Korea

[*] Corresponding author: jedlinsk@agh.edu.pl

Transient oxidation of β-NiAl and the influence of various factors, especially RE-additions, on its course have been the subject of numerous studies [1-7,12-14,17,18,22,31-56]. These studies investigated changes in the morphology and microstructure of the formed scale under various conditions and during various stages of oxidation. The influence of reactive elements was also qualitatively and quantitatively compared, most often taking into account their type (which element?), form, quantity, and incorporation route. The influence of other elements was also investigated to some extent. Furthermore, attempts were made to model and quantify the degree of phase transformation of transient Al_2O_3 oxides into the alpha phase, as well as the impact of this transformation on subsequent stages of the oxidation process.

Although, the reported in these papers results have significantly improved our understanding of the process of formation of α-Al_2O_3, it still cannot be considered sufficiently satisfactory. This is primarily due to the fact that the overwhelming majority of experimental work did not refer to successive stages of evolution, but, most often, to a single, arbitrarily selected exposure conditions. It is worth noting that the transformation of transient Al_2O_3 phases into α-Al_2O_3 which occurs in scales during the initial stages of oxidation is also of interest in the field of catalysis (γ-Al_2O_3 is considered a very good support for catalysts, e.g., Pt). and sometimes during studying the early stages of oxidation of alumina formers, the achievements are applied that have been obtained in catalysis research (e.g. [57-61]). It is important to emphasize that this transformation is accompanied by a structural rearrangement resulting in approximately a 10% volume reduction. This is believed to be the cause of patches and cracks in the scale.

As already suggested elsewhere [22,62,63], a full understanding of how the scale grows and how the protective α-Al_2O_3 scale develops requires extensive and systematic study of the early oxidation stages, because the scales on β-NiAl evolve. Therefore, consecutive stages of the scale development should be followed in terms of the scale microstructure, morphology, phase composition, preferred location of the oxide growth. Such a combination of results would provide reliable evidence of the scale growth mechanism for the whole relevant period of the scale development, and not only for deliberately chosen conditions. It is worthwhile noting that a systematic approach helps avoid arriving at misleading conclusions and differentiating between the influence of the additions on the change of the scale growth mechanism and on the rate of the scale evolution.

Taking the above into account a comprehensive research effort has been made to improve understanding of the scale formation process on unmodified and yttrium-implanted β-NiAl compound.

This paper reports the results concerning the evolution of the scale morphology and phase composition.

2. Materials and experimental

The β-NiAl intermetallic compound was obtained by the vacuum melting of metals of electrolytic purity. Analysis of its chemical composition showed that it contained (in wt.%): Ni – bal., Al – 28.7, Si – 0.07, Fe – 0.07, Ti – 0.04, and Cr – 0.0092.

The cylinder-shaped ingot (bar) having diameter of 15 mm was annealed at 1100°C for 24 hs under an argon atmosphere (purity 99.998%). The thin oxide layer formed at its external surface was subsequently removed though abrasion. Samples in the form of 0.9 mm-thick discs were cut from the ingot. Their further preparation relied on grinding and polishing their surfaces with 600 SiC grit and 1 μm diamond paste, respectively, and degreasing in water with detergent and acetone. Just before oxidation exposure, the specimens were ultrasonically cleaned in acetone.

Ion implantation was chosen as the method of introducing the addition for the following reasons: i) it allows for enrichment of only the outermost layer of the material with a thickness of several dozen nanometres (without affecting its interior); ii) it allows for good control of the amount of the introduced addition and its distribution on the depth scale as well as uniform enrichment over the surface; iii) REE was demonstrated to occur when this method was used for yttrium for a period sufficient from the point of view of the problem under investigation [5-7].

Yttrium was implanted into the entire surface layer of some specimens or of their parts, the remaining part being left unmodified. This procedure allowed for a single sample to contain both types of materials. The following implantation parameters were used: ion beam energy of 70 keV and dose of 2×10^{16} ions/cm^2. The distribution of implanted Yttrium determined using SIMS in-depth profiling has been reported elsewhere [36].

A series of oxidation exposures in oxygen were carried out at 1100°C for 3 min, 7 min, 15 min, 1 h, 6 h and 24 h. Samples were introduced rapidly into a constant-temperature zone in a horizontal tube furnace, previously heated to the oxidation temperature. After exposure, the samples were rapidly removed from the reaction temperature to ambient temperature, where cooling occurred.

Evolution of the scale, in terms of its morphology and phase composition, was determined by means of SEM, Low-Angle X-Ray Diffraction (LA-XRD) and Photoluminescence Spectroscopy (PLS).

3. Results

3.1. Introductory remarks

A series of oxidation exposures in oxygen were carried out at 1100°C for six different periods, from 3 min to 24 h for both studied materials in order to follow the consecutive stages of scale formation. LA-XRD and PLS applied to determine the phase composition of scales exhibited different lateral resolution: that of the latter was of down to ca. 1 μm, which is significantly better than that of LA-XRD which averages the target response over surface area of order of several square millimetres. The photoluminescence spectra in frequency (in cm^{-1}) ranges corresponding to the possible presence of alumina phases were attributed to θ-Al_2O_3 and α-Al_2O_3 as proposed elsewhere [33, 34]:

a strong stress-free α-Al_2O_3-related doublet appears at nominal frequencies of 14,432 and 14,402 cm^{-1}, whereas that associated with θ-Al_2O_3 is at 14,530 and 14,610 cm^{-1}. Due to such a clear difference, possible effects related to the occurrence of stresses in the alumina phases, related primarily to the transformation of the transition phases into the alpha phase (structural stresses) and to the rapid cooling of the reacting system from the reaction temperature to the ambient temperature (thermal stresses), resulting in the shift of doublets, do not prevent the phase identification during the analysis. The presence of γ-Al_2O_3 manifests itself less spectacularly in PLS spectra and may frequently only be demonstrated as a contribution to the θ-related doublet at lower luminescence frequencies (in cm^{-1}), affecting its shape. Wherever it was required, different morphology and/or microstructure details were analysed by focussing the incident laser beam on them. The analysed regions are always marked by circles of relevant size in SEM micrographs.

Regarding the LA-XRD results, it should be noted that: (i) the oxide-related maxima collected were expressed in the form of interplanar distances ($d_{hkl}'s$) observed for various scales and attributed to possible phases according to the JCPDS Database; (ii) the maxima were frequently fairly broadened and the determined $d_{hkl}'s$ were slightly different with respect to those reported in the JCPDS database; (iii) the maxima which may have corresponded to both transient oxides and α-Al_2O_3 as well to β-NiAl are not reported, and relatively few maxima are left to identify phases (at least to distinguish between transient Al_2O_3-oxides and α-Al_2O_3) after such a procedure for further interpretation; (iv) despite using the very low angle of incident beam, the non-conclusive X-ray patterns were obtained from scales formed upon shorter exposures (3 min and 7 min) of both materials and are therefore not reported.

Concerning the PLS spectra, it should be noted that sometimes the maxima exhibited more complex shapes than expected for typical θ-Al_2O_3- and α-Al_2O_3-related 'single' doublets because of very fine grains of initially growing scales which resulted in the detection of the superimposed luminescence signals from different adjacent grains. The different strain of these grains can be a reason for the shifts and shapes observed. In the case of multilayered scales, the same effect might occur. In such cases, the fairly good spatial resolution of the PLS was still not sufficient to separate these signals. Nevertheless, despite this inconvenience, it was possible to distinguish and identify the θ and α alumina phases. Therefore, the PLS as-received raw spectra are shown which were not further processed in terms of the removal of background. The analysed regions are always marked by circles of relevant size in SEM micrographs. It should be noted that it was not possible to obtain a luminescence spectrum that would allow for the identification of the sought phases for scales on the yttrium-implanted material oxidized in the shortest time (3 min, 7 min, 15 min). The lack of signal in LA-XRD and PLS analyses after the shortest exposure times is related to the properties of the scale (insufficient thickness, insufficiently developed structure).

3.2. Results for non-implanted β-NiAl

A surface view of the scales formed upon the oxidation exposures of non-implanted β-NiAl is shown in Figs. 1-6 together with the PLS spectra corresponding to the marked regions. The results of LA-XRD maxima are summarised in TABLE 1.

It follows from Fig. 1A-C (exposure for 3 min) that at the very beginning of the reaction of non-implanted material rather flat scale was formed, which did not exhibit any particular features except for some darker-appearing spots of sub-micron size and rather regular shapes (Fig. 1B, 1C). Development of the latter was studied in detail by Oquab and Monceau [35] and attributed to the secondary electron image contrast associated with

TABLE 1

Collected results of Low-Angle X-Ray Diffraction analysis of oxide scales formed upon oxidation exposure at 1100°C of non-implanted (ni) and Yttrium-implanted (iY) β-NiAl: only maxima which enable identification of phases are shown (X – presence of the maximum; w – weak)

d_{hkl} [Å] – measured	ni 15 min.	ni 1 h	ni 6 h	ni 24 h	iY 15 min.	iY 1 h	iY 6 h	iY 24 h	Possible Phases
3.48-3.50	X	X		X					**α(3.48)**
3.48								X	**α**
2.88	X				X	X		X-w	**θ**
2.73/2.74	X	X				X			**δ/θ**
2.44	X				X				**θ**
2.31					X				**δ/θ**
2.25		X							**δ/θ(2.26)**
2.09	X	X	X-w	X			X-w	X	**α**
1.92					X				**θ**
1.79/1.80			X-w		X		X-w		**δ/θ (γ)**
1.72		X							**θ(?)**
1.70/1.71		X							**δ(?)**
1.4597					X				θ
1.375	X			X				X	**α**
Identified oxide phases	**θ, δ/θ, α**	**δ/θ, α**	**α, δ/ θ**	**α**	**θ, δ/θ**	**θ, δ/θ**	**α, δ/θ**	**α, θ**	

Note: for oxidation times up to 15 min, no diffraction maxima originating from oxides were observed for both materials

the formation of cavities at the scale-substrate interface already at very initial stages of the exposure, even before reaching the reaction temperature. They appear to be preferentially aligned along the substrate grain boundaries and polishing marks. In addition, some minor irregularities of the scale were only locally observed under very high magnification as oxide flakes on a relatively smooth surface (Fig. 1C).

The PLS spectrum shown in Fig. 1D, which is representative of the entire scale, indicates that the majority of the scale was composed of transient oxide θ-Al_2O_3 and only small maximum related to α-Al_2O_3 appeared, corresponding to the minor content of this phase. The relatively high background of the PLS signal has to be noted as well as the presence of increased luminescence at a frequency of ca. 14 300 cm^{-1} which cannot be ascribed to photoluminescence of any of the alumina phases. Moreover, the broadening of the lower θ-related maximum may indicate the presence of some γ-Al_2O_3 oxide. The latter, having a shape of small hump, can hardly be attributed to the background.

Considerably less uniform morphology of the scale surface resulted from oxidation for 7 min, as shown in Fig. 2A-2F. It should be noted that: (i) bright-appearing round patches ('spots') developed but their surface fraction strongly depended on the substrate grain on which the scale was formed (Fig. 1A, 1B); (ii) further growth of interfacial cavities occurred as it follows from the comparison of the size of dark-appearing spots in Figs. 2C and 1B (the same magnification); (iii) the surface fraction of patches coincided with the surface fraction of dark spots, the higher the former the higher the latter (Fig. 2B); (iv) in some patches in 'highly patched' regions small ridge-like oxide protrusions appeared (Fig. 1D); (v) in regions with a low fraction of patches, some radial cracks were formed (Fig. 1E); (vi) the size of the grains observed at the scale surface was very fine, up to 0.15 μm (Fig. 1F: note magnification of 100 000).

The phase composition of the scale (Fig. 2G) was also found to depend on the region and sub-region of the scale. In 'highly patched' regions, α-Al_2O_3 predominated in the centre of the patch with ridge-like protrusions and only very small luminescence of θ-Al_2O_3 was detected (curve 4 in Fig. 2G). Outside of patches in this region, similar PLS intensity was observed for both, α and θ phases (curve 2 in Fig. 2G). In 'low-patched' regions, in the sub-region with initial patches and cracks, α- and θ-oxides appeared but α one prevailed (curve 3 in Fig. 2G). For similar reasons to those mentioned above, the presence of γ-Al_2O_3 cannot be excluded in this case. In the patch-free sub-region, however,

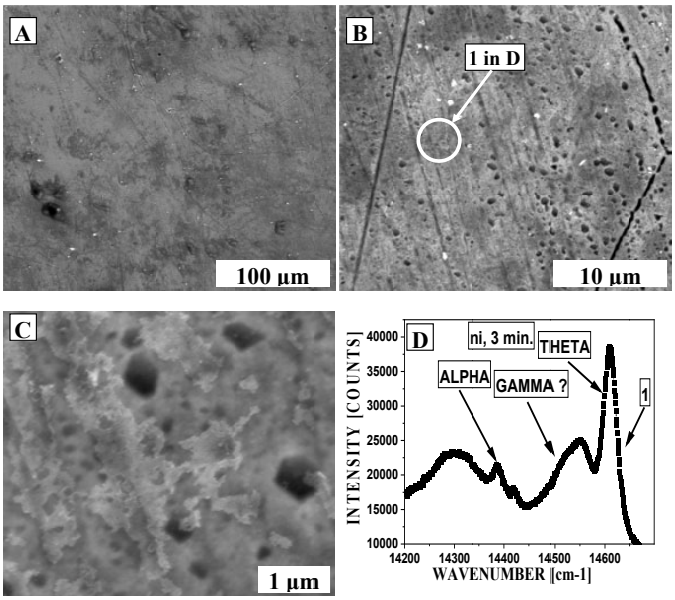

Fig. 1. Surface (A-C) and PLS spectra (D) of the scale formed on non-implanted β-NiAl upon oxidation exposure in oxygen for 3 min. at 1100°C. Scale marks are numbers in white boxes which widths correspond to size given by numbers. White circles in the SEM images indicate the corresponding PLS analysis location and the size of the analyzed area

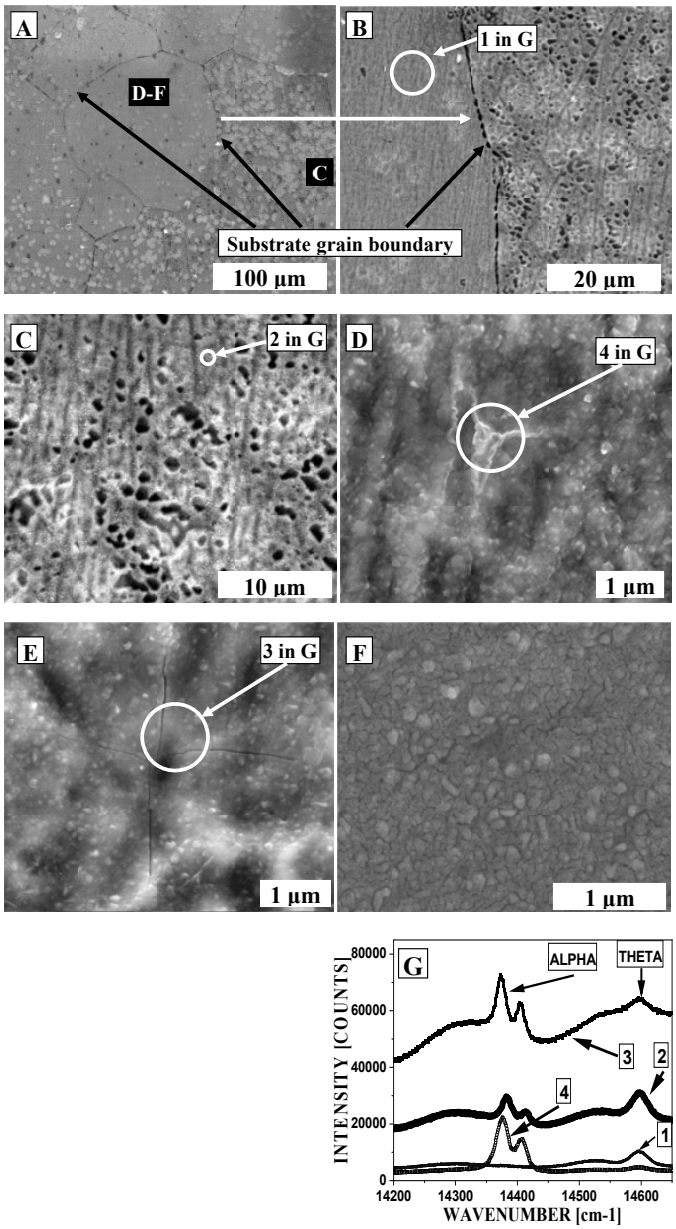

Fig. 2. Surface (A-F) and PLS spectra (G) of the scale formed on non-implanted β-NiAl upon oxidation exposure in oxygen for 7 min. at 1100°C. Scale marks are numbers in white boxes which widths correspond to size given by numbers. White circles in the SEM images indicate the corresponding PLS analysis location and the size of the analyzed area

only θ-Al_2O_3 was clearly detected (curve 1 in Fig. 2G). These results show that significantly more α-Al_2O_3 developed in 'highly patched' regions than in 'low-patched' ones.

The different extent of patches is even more clearly visible in scales formed during more prolonged oxidation, 15 min as shown in Fig. 3A. Moreover, their surface fraction strongly depended on the substrate grain on which the scale appeared. Hence, again two types of regions can be distinguished: 'highly patched' and 'low-patched'. In the former ones, well-developed cracks were observed with oxide filling them (Fig. 3B). In 'low-patched' regions, smaller cracks were found, without any indications of the 'in-crack' oxide (Fig. 3C). The fine-grained scale of the grain size of up to 0.25 μm, but usually lower, was observed at the scale surface (Fig. 3D).

The LA-XRD analysis revealed the presence of both types of aluminium oxides, the transient (θ and possibly δ) and α-Al_2O_3. The PLS results showed, however, that α-Al_2O_3 was essentially detected in the centres of patches in 'highly patched' regions (curve 1 in Fig. 3E), while a similar intensity of luminescence from both phases was observed outside the centres (curve 2 in Fig. 3E). Although in 'low-patched' regions, but in the vicinity of cracks, α-Al_2O_3 predominated, the θ-Al_2O_3-related component of the PLS spectrum was noticeable (curve 4 in Fig. 3F). Virtually no α-phase was found far from cracks in the latter region, θ-phase being the prevailing aluminium oxide (curve 3 in Fig. 3F). It should be noted that the intensity of the PLS signal was much stronger in 'low-patched' regions than in 'highly patched' ones, as demonstrated in Fig. 3 E and F.

Only α-Al_2O_3 was detected in scale using PLS method during oxidation for 1 h (Fig. 4J), independently of the analysed

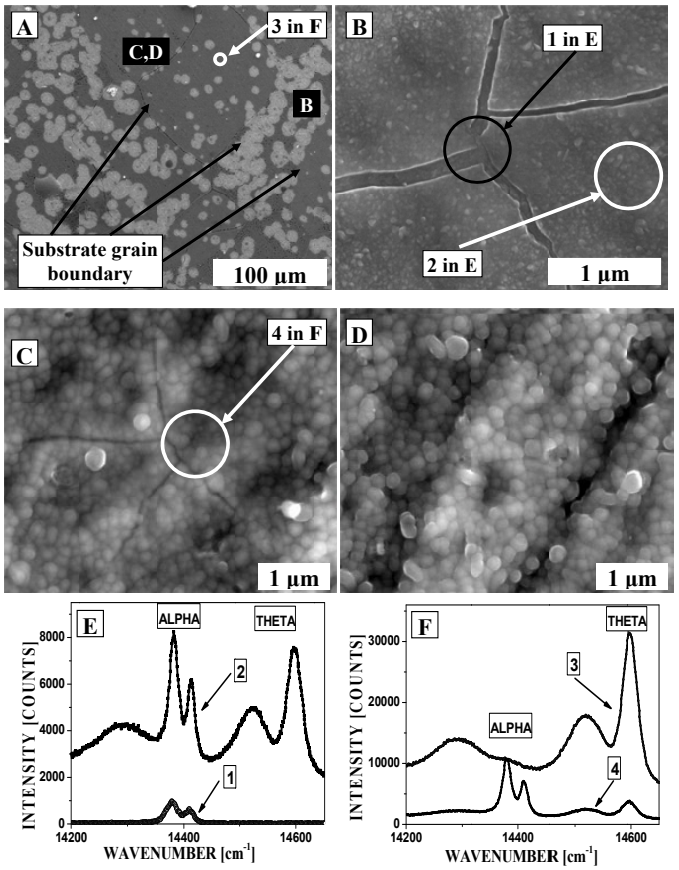

Fig. 3. Surface (A-F) and PLS spectra (G) of the scale formed on non-implanted β-NiAl upon oxidation exposure in oxygen for 15 min. at 1100°C. Scale marks are numbers in white boxes which widths correspond to size given by numbers. White circles in the SEM images indicate the corresponding PLS analysis location and the size of the analyzed area

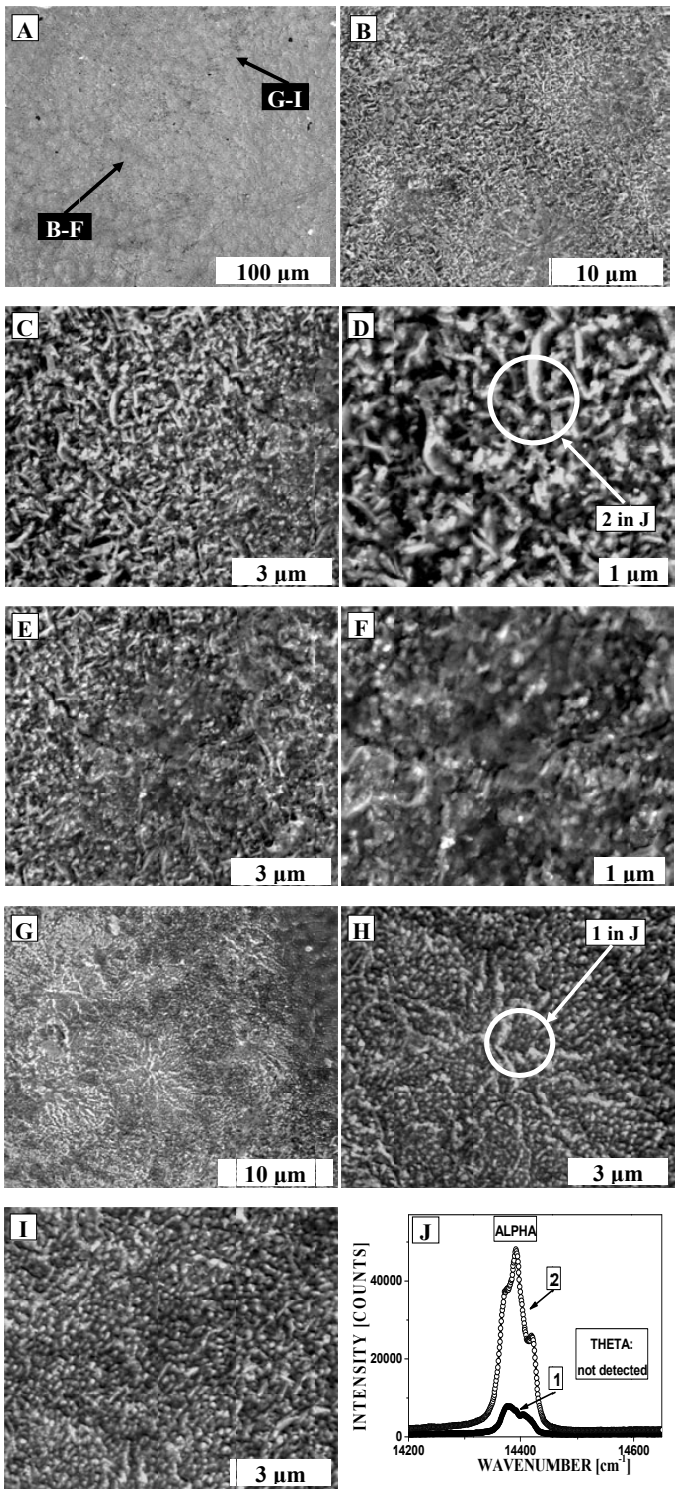

Fig. 4. Surface (A-I) and PLS spectra (J) of the scale formed on non-implanted β-NiAl upon oxidation exposure in oxygen for 1 hr at 1100°C. Scale marks are numbers in white boxes which widths correspond to size given by numbers. White circles in the SEM images indicate the corresponding PLS analysis location and the size of the analyzed area

region. However, some maxima related to transient alumina phases were also found in the LA-XRD spectrum (TABLE 1). It appears that more grains exhibiting different strain contributed to the photoluminescence spectra, making them more complex and broadened than typical α-related doublets. The 'brighter-appearing' and 'darker-appearing' regions shown together in Fig. 4A, and separately under higher magnifications in Fig. 4B-F and 4G-I respectively, differed in terms of their surface morphology. In the 'darker-appearing' regions which constituted minor surface fraction, a fairly significant part of the scale was composed of blade-like grains (platelets) (Fig. 4B-D), while patches with cracks were observed in the other regions (Fig. 4B, E, F). Only remnants of the 'blade-like' grains which nearly lost their platelet shape developed in 'brighter-appearing' regions (Fig. 4G, I) and patches with radial cracks and oxide growing in them and protruding at the surface were found (Fig. 4G, H). The PLS-spectra shown in Fig. 1J, correspond to the most and least developed stages of scale evolution, but as mentioned previously, always consisting of α-Al_2O_3.

Fairly similar results were obtained for material oxidized for 6 hs, as shown in Fig. 5. The only difference is that scale further evolved and were composed of laterally growing patches and the ridges started to form a web-like surface morphology (Fig. 5A-D). Still remnants of oxide platelets were present between patches and in patches between the ridges (Fig. 5E). Again, α-Al_2O_3 was only detected using the PLS method in the entire scale, independently of whether it was in patches, ridges or remnants of platelets (Fig. 5F), but some indication of the presence of transient oxides appeared in the LA-XRD spectra.

Two regions appeared at the surface of the scale formed upon oxidation for 24 hs: the 'brighter-appearing' regions with more developed web-like morphology (higher surface fraction and larger ridges) and 'darker-appearing' ones with less developed web-like morphology (Fig. 6A-C). Frequently, spallation of the scale occurred (Fig. 6A). In this case, α-Al_2O_3 was essentially detected in the entire scale, independent of the analytical tool applied (Fig. 6D, TABLE 1).

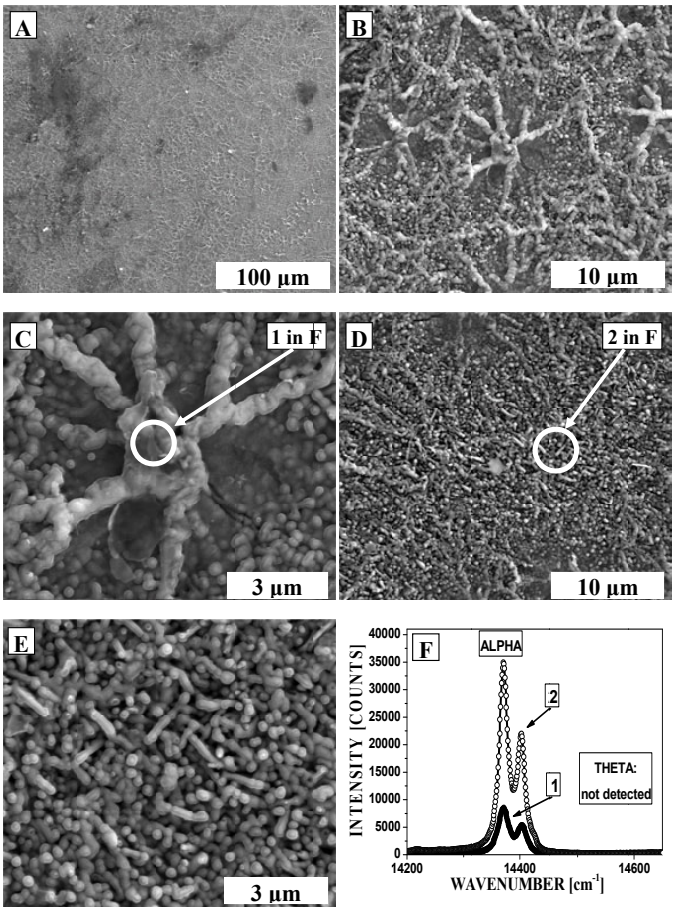

Fig. 5. Surface (A-E) and PLS spectra (F) of the scale formed on non-implanted β-NiAl upon oxidation exposure in oxygen for 6 hrs at 1100°C (A-D region with patches, E – region outside of patches). Scale marks are numbers in white boxes which widths correspond to size given by numbers. White circles in the SEM images indicate the corresponding PLS analysis location and the size of the analyzed area

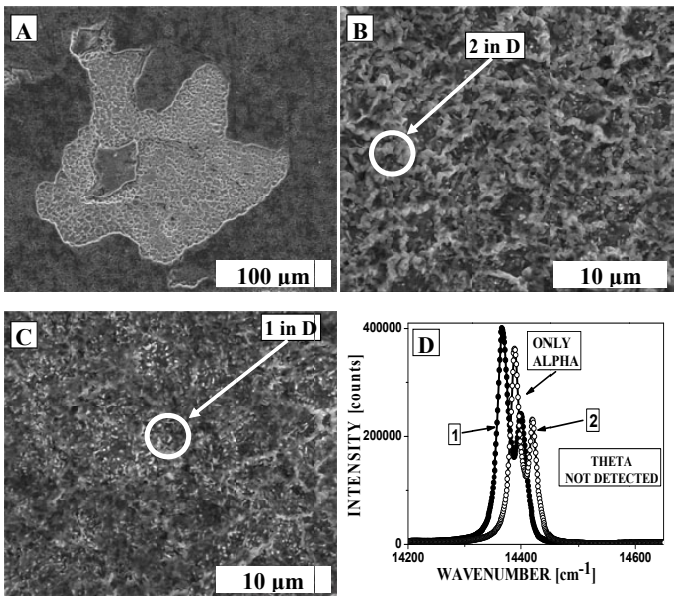

Fig. 6. Surface (A-C) and PLS spectra (D) of the scale formed on non-implanted β-NiAl upon oxidation exposure in oxygen for 24 hrs at 1100°C (B, C – higher magnification of regions with well- and less-developed web-like surface morphology, respectively). Scale marks are numbers in white boxes which widths correspond to size given by numbers. White circles in the SEM images indicate the corresponding PLS analysis location and the size of the analyzed area

3.3. Results for Yttrium-implanted β-NiAl

A surface view of the scales formed upon the oxidation exposures of Y-implanted β-NiAl is shown in Figs. 7-12, completed for the more prolonged oxidation (1-24 hs) together with PLS spectra corresponding to the marked regions. In TABLE 1, the results of LA-XRD maxima are summarised.

It follows from Fig. 7A-C (exposure for 3 min) that at the very beginning of the reaction of non-implanted material, fairly flat scale was formed with only very few darker-appearing spots of sub-micron size and rather regular shapes, similar to those found on non-implanted material (Fig. 1B, C). The 'white-

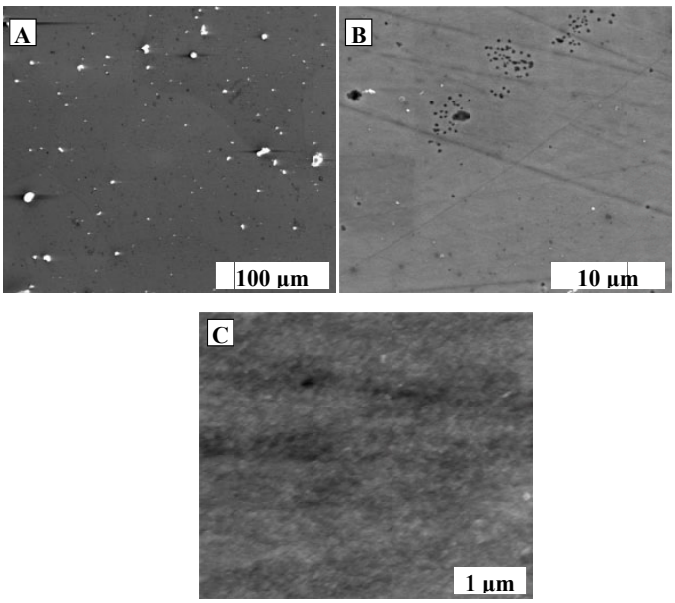

Fig. 7. Surface of the scale formed on Yttrium-implanted β-NiAl upon oxidation exposure in oxygen for 3 min. at 1100°C. Scale marks are numbers in white boxes which widths correspond to size given by numbers

appearing' contaminations visible at the scale surface (Fig. 7A) should be considered as artefacts.

Rather flat and very fine-grained (0.15 µm and less) scale resulted from oxidation for 7 min, as shown in Fig. 8A-C. The higher than in previous case surface fraction of very small dark-appearing spots was found (Fig. 8A).

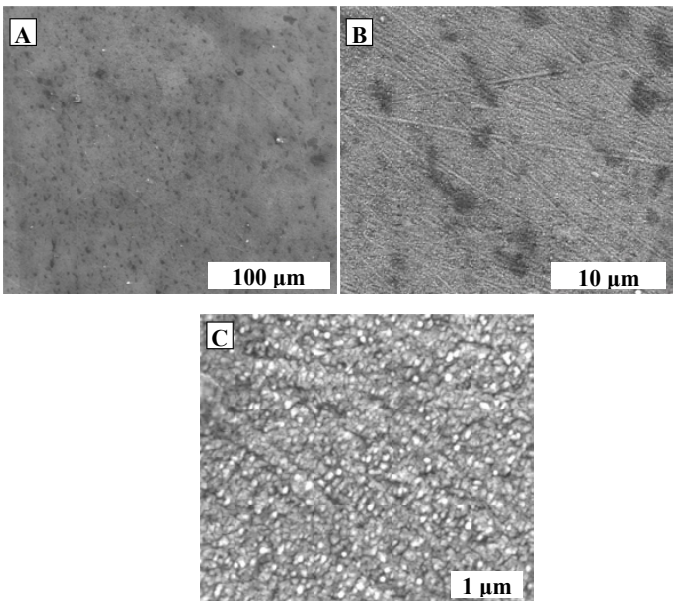

Fig. 8. Surface of the scale formed on Yttrium-implanted β-NiAl upon oxidation exposure in oxygen for 7 min. at 1100°C. Scale marks are numbers in white boxes which widths correspond to size given by numbers

The fairly flat scale was formed even upon oxidation for 15 min (Fig. 9A-C), with indication of the initial stage of development of 'blade-like' surface morphology only observed clearly under rather high magnification (Fig. 9C).The size of 'dark-appearing' spots further grew. Only transient aluminium oxides, mostly θ-Al_2O_3, were detected in scale using LA-XRD (TABLE 1).

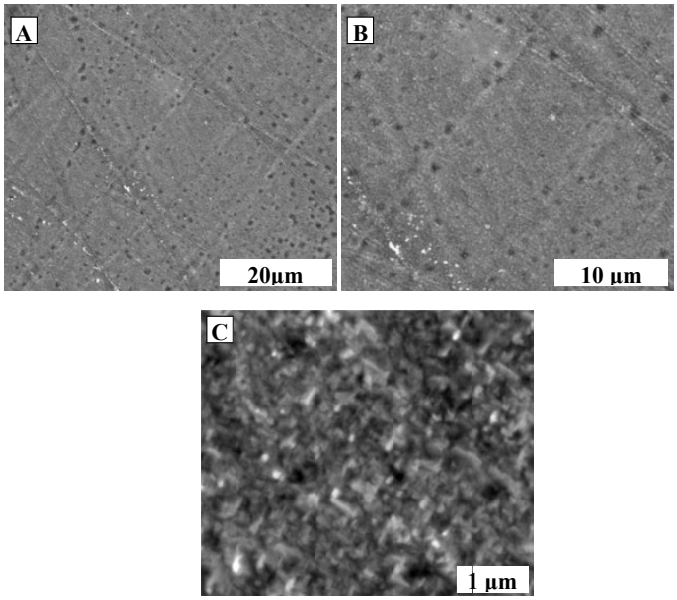

Fig. 9. Surface of the scale formed on Yttrium-implanted β-NiAl upon oxidation exposure in oxygen for 15 min. at 1100°C. Scale marks are numbers in white boxes which widths correspond to size given by numbers

The 1 h oxidation brought about numerous, relatively large patches in the scale in which patch-free regions still predominated, as shown in Fig. 10A and B. In the latter regions, well-developed oxide platelets were found at the scale surface using higher magnification (Fig. 10C-E). The PLS spectra indicate that α-Al_2O_3 essentially developed in patches (curve 2 in Fig. 10F), whereas θ-Al_2O_3 prevailed in patch-free regions (curve 1 in Fig. 10F). Neither PLS nor LA-XRD analyses did provide results indicating the presence of the α-Al_2O_3 phase.

The scale formed upon 6 hs of oxidation is shown in Fig. 11 together with corresponding PLS spectra. Similarly to that observed after 1 h-exposure, the scale exhibited two clearly different regions: one with surface covered by oxide platelets consisting of α-Al_2O_3 (curve 1 in Fig. 11E) and the second being patches which were essentially composed of θ-Al_2O_3 (curve 3 in Fig. 11E). However, in patches and close to the border between two regions both phases were detected (curve 2 in Fig. 11E). From the results of LA-XRD it follows that two types of alumina phases appeared in the scale: transient and α-Al_2O_3 ones.

According to the PLS results, 24 hour-oxidation was necessary to produce α-Al_2O_3 as the only phase in the scale on Y-implanted material (Fig. 12H) despite the different scale morphology (Fig. 12A-G). However, the LA-XRD results still demonstrated the presence of weak maximum, which may be attributed to the transient oxide θ-Al_2O_3 (TABLE 1). It shows again that depending on the analytical tool applied slightly

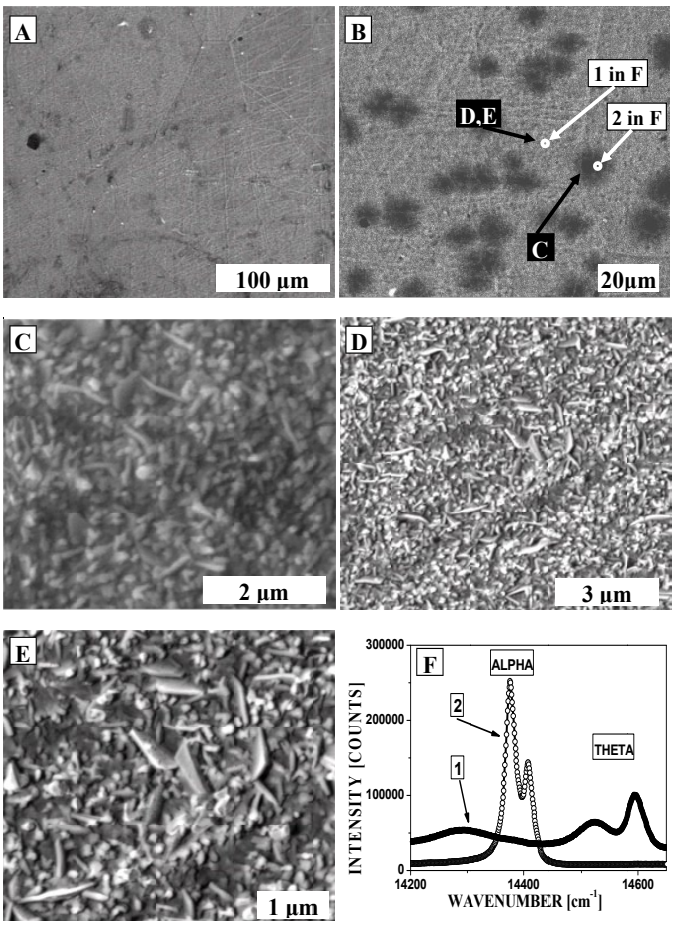

Fig. 10. Surface (A-E) and PLS spectra (F) of the scale formed on Yttrium-implanted β-NiAl upon oxidation exposure in oxygen for 1 hr at 1100°C. Scale marks are numbers in white boxes which widths correspond to size given by numbers. White circles in the SEM images indicate the corresponding PLS analysis location and the size of the analyzed area

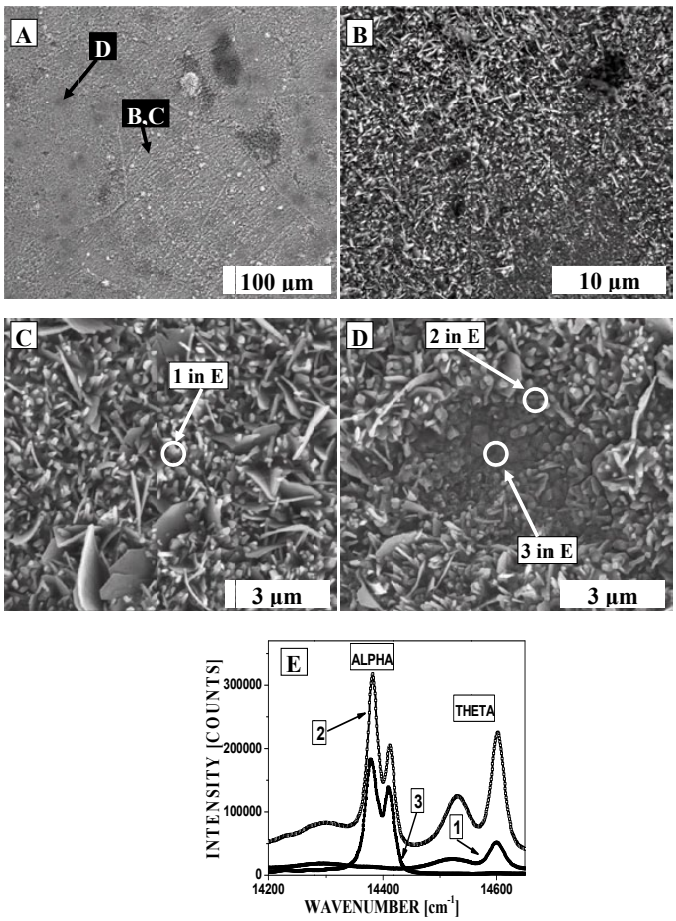

Fig. 11. Surface (A-D) and PLS spectra (E) of the scale formed on Yttrium-implanted β-NiAl upon oxidation exposure in oxygen for 6 hrs at 1100°C. Scale marks are numbers in white boxes which widths correspond to size given by numbers. White circles in the SEM images indicate the corresponding PLS analysis location and the size of the analyzed area

different results can be obtained concerning the phase composition of the oxide layer. The scale exhibited regions with different stages of development of web-like morphology and the extents of patch- and web-like morphology-free regions. It can be illustrated though a comparison of the scale surface shown in Fig. 12A, E, F and in Fig. 12B, C, D which correspond to such regions. In the former regions, some remnants of oxide platelets can still be found (Fig. 12D and G). However, they do not exhibit different scale phase composition with respect to the patches and web-like regions.

4. Discussion

The scales formed on polycrystalline non-implanted and Yttrium-implanted β-NiAl appear to exhibit very similar consecutive stages of their evolution in terms of morphology and phase composition, and only minor differences between both materials. However, the implanted addition affects the rate of the scale evolution which, in addition, clearly depends on the substrate grain. The following common consecutive stages can be inferred from the results obtained for exposures at 1100°C ranging from 3 min to 24 hours:

1. Formation of rather flat scale without any special features and with some spots related to the local delamination at the scale-substrate interface which begins at very early stages of the exposure, in particular on Y-free material (Figs. 1, 7, 8). This scale essentially consists of transient aluminium oxides;
2. Local development of round patches with increased amounts of α-Al_2O_3 surrounded by oxide exhibiting more or less distinct blade-like (platelets) morphology of the surface where transient oxides still predominate (Figs. 2, 10, 11);
3. Lateral growth of patches and formation of cracks in patches in which successively 'new' oxide grows filling them and appearing as ridges at the scale surface. In the oxide outside the patches transient oxides still are present, but the amounts of α-Al_2O_3 successively increases and the blade-like morphology disappears, whereas in patches α-Al_2O_3 predominates, being the only oxide detected in ridges (Figs. 3, 12);

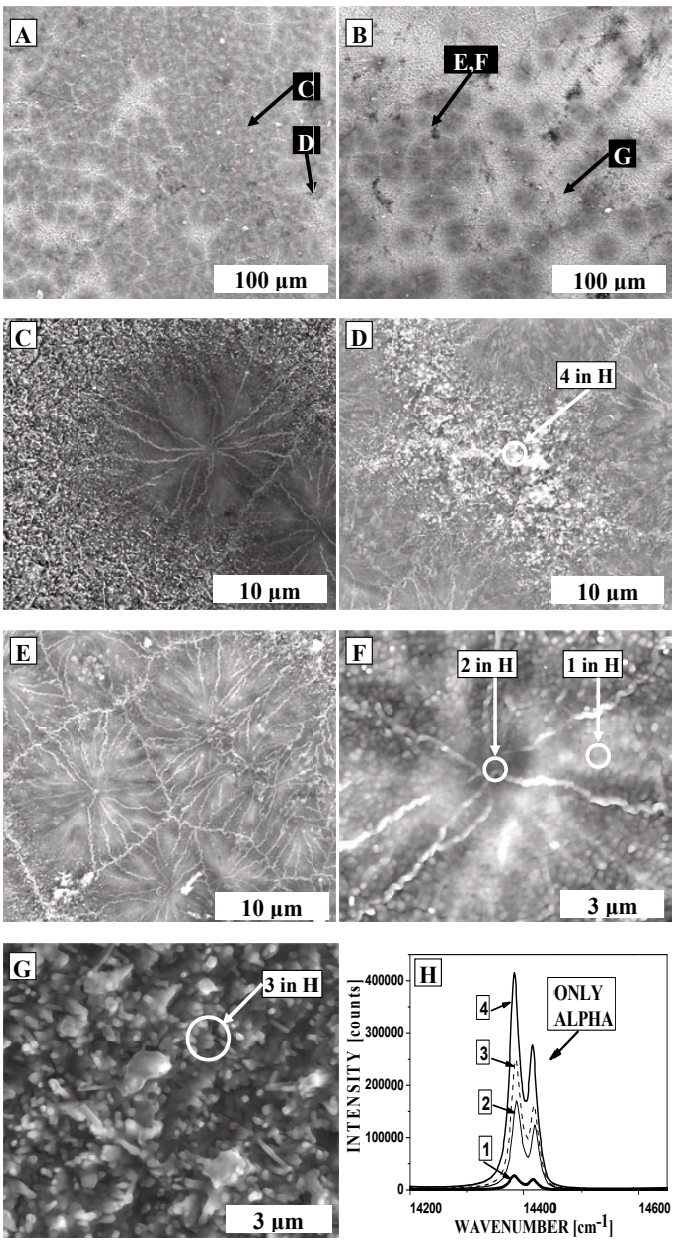

Fig. 12. Surface (A-G) and PLS spectra (H) of the scale formed on Yttrium-implanted β-NiAl upon oxidation exposure in oxygen for 24 hrs at 1100°C. Scale marks are numbers in white boxes which widths correspond to size given by numbers. White circles in the SEM images indicate the corresponding PLS analysis location and the size of the analyzed area

4. Co-existence of regions exhibiting different morphology in terms of surface coverage by patches and ridges successively forming web-like surface morphology but consisting of α-Al_2O_3 with possibly small amounts of transient oxides on Y-implanted material (Figs. 4-6, 12).

In general, the above is consistent (in the part that is the subject of the research reported here) with one of the oxidation routes proposed in the only attempt to integrate the description of scale evolution on alumina formers, taking into account the phase composition of the scale; the scale growth mechanism; the scale morphology and microstructure, and various interfacial phenomena [11].

TABLE 2 contains the collected information concerning the relationship between the identified evolution stages of the scale and the exposure conditions for both materials studied. The numbers used in TABLE 2 correspond to these applied to the above described stages. It is worth noting that under the studied conditions, no oxide phases containing Ni as a component were found in the scale.

TABLE 2

Evolution stages observed in scales formed on non-implanted and Yttrium-implanted β-NiAl upon oxidation exposure at 1100°C (numbers refer to numbered list in Chapter 'Discussion')

Exposure time	β-NiAl (non-implanted)	Y-implanted β-NiAl
3 min.	1	1
7 min.	2	1
15 min.	3	2
1 hr	4	2
6 hrs	4(1)	3
24 hrs	4	4(2)

(1) LA-XRD results but not PLS ones indicated presence of weak α-Al_2O_3-related maximum

(2) LA-XRD results but not PLS ones indicated presence of weak θ-Al_2O_3-related maximum

As can be clearly seen from TABLE 2, implanted Yttrium significantly retarded the scale evolution, mainly by impeding the phase transformation of transient aluminium oxides into α-Al_2O_3, and thereby, development of the latter. Indeed, in the case of non-implanted β-NiAl, 1-hour exposure was sufficient to result in the scale built of the protective α-Al_2O_3 layer, while on the Y-implanted material even upon 6 hs oxidation considerable amounts of transient θ-Al_2O_3 oxide still appeared. The results obtained for non-implanted β-NiAl oxidized for 6 h and for Y-implanted β-NiAl oxidized for 24 hs are not unambiguous in terms of the scale phase composition, because the PLS spectra indicated no presence of transient oxides while in the LA-XRD ones the weak maximum related to θ-Al_2O_3 is still present.

The latter effect may be a consequence of a general trend observed relying on the highly local nature of the scale evolution. Both, the scale morphology and phase composition vary substantially from region to region. However, no strict coincidence was observed between the scale morphology and phase composition. It means that although at the early oxidation stages the blade-like morphology seems to correspond to transient aluminium oxides, the remnants of this morphology are still present in scales comprising essentially α-Al_2O_3. It might be, however, the case that the thickness of transient oxides-containing sub-layer of the scale is too low to contribute considerably to the PLS spectrum. Nevertheless, the predominant phase of α-Al_2O_3 should decisively affect the protective properties of such scales.

The obtained results indicate that if the materials are subjected to thermal cycles, the additional factors related to the phase composition of the scales should be taken into account during the interpretation procedure. For instance, the first of the

1-h cycles (which is the case for majority of reported results of experiments) is applied to different scales in terms of their phase composition which may result in the different responses of the cycled system. The latter consists of β-NiAl and α-Al_2O_3 for non-modified materials and of β-NiAl and a mixture of α-Al_2O_3 and θ-Al_2O_3 for Yttrium-implanted β-NiAl. The higher coefficient of thermal expansion of θ-Al_2O_3 than that of α-Al_2O_3 ([64]) may contribute to the level of stresses generated, while the interfacial strength between these two phases should play a role in the manner of their relief. However, the longer the cycle duration the more homogeneous scale in terms of its phase composition is subjected to the cooling-heating cycles.

It should be added that this study did not address the generation and distribution of residual stresses in α-Al_2O_3 oxide. This would require a much larger number of PLS analyses, in particular using linear and mapping modes, to achieve adequately representative results.

An interesting issue for possible further research, at this stage being beyond the main scope of planned research, may be to attempt to explain what factors decisively influence the non-uniform distribution on the scale surface of the sites where the transformation of transient aluminium oxides into the alpha phase begins. This effect manifests itself upon SEM observations as the presence of patches and their non-uniform surface fraction in different regions. Certainly one of the most important factors is the orientation of the substrate grains. Fig. 6 illustrates through different positions of the doublet maxima for α-Al_2O_3 that the stress level varies from region to region.

5. Concluding remarks

The systematic following of scale evolution on non-implanted and Yttrium-implanted polycrystalline β-NiAl grown at 1100°C in oxygen in terms of its morphology and phase composition allowed for the inferring that the implanted addition affects the rate of evolution rather than its mechanism. It is because of the similar consecutive stages as far as both features are concerned but that they developed later on Yttrium-implanted material.

However, the very local nature of the scale evolution was observed and the substrate composition and/or its modification was not the only factor affecting the rate of evolution. The other important factor was the substrate microstructure. The consecutive stages developed with different rates on different substrate grains. Hence, the superposition of both factors, surface modification by ion implantation of Yttrium and substrate grain orientation should be taken into account in the interpretation of the results obtained.

No unambiguous coincidence between the scale morphology and its phase composition was found, despite the tendency to attribute the blade-like morphology to transient aluminium oxide phases only. The latter was found to be necessarily valid in scales formed upon more prolonged oxidation but still at its transient stage.

The reported here results imply that it is necessary to complete the obtained description of the early stages of oxidation with more detailed studies of: (i) the microstructure, using transmission electron microscopy (TEM), and (ii) the mechanism of scale growth, using a combination of two-stage oxidation exposures, with that enriched in oxygen isotope ^{18}O as a tracer, and secondary ion mass spectrometry (SIMS). The results of such studies, the initial part of which has already been reported [13], will be published soon.

It should also be noted that the transient oxides are fairly stable in scales, in particular on Yttrium-implanted β-NiAl (even up to 6 hs and, perhaps, to 24 hours) which may affect the response of the scale-substrate system to thermal stresses imposed during thermal cycling exposure.

The following general conclusion and warning can be drawn from the obtained results: the duration of exposure during the first oxidation cycle upon thermal cycling may be significant. Various scales may experience the first so-called thermal shock, including those in which a steady-state protective scale has not yet formed. The response of the reacting system and, importantly, the subsequent course of oxidation may depend on this.

Acknowledgements

Prof. Jan Bonarski† (IMiIM PAN, Kraków), and Mr. Mariusz Konopka (AGH, currently: WS-Atkins Polska Sp. z o.o. Warszawa) are kindly acknowledged for assistance in, respectively: LA-XDR analyses and oxidation exposures. The financial support of the Polish Minister of Science and Higher Education (Grant No. N N507 444934) is gratefully acknowledged. The research was partially financed by the "Excellence Initiative – Research University" program (IDUB) at AGH University of Krakow and from the subsidy of the Minister of Science and Higher Education for the AGH University of Kraków.

REFERENCES

[1] R. Hutchings, M. H. Loretto, R. E. Smallman, Oxidation of intermetallic compound NiAl, Metal Science **15** (1), 7-13 (1981). DOI: https://doi.org/10.1179/msc.1981.15.1.7

[2] J.L. Smialek, Oxide Morphology and Spalling Model for NiAl. Metallurgical Transactions A **9A**, 309-320 (1978). DOI: https://doi.org/10.1007/BF026463803

[3] H.M. Hindam, W.W. Smeltzer, H.M. Hindam, W.W. Smeltzer, Growth and Microstructure of alpha- Al_2O_3 on beta-NiAl. J. Electrochem. Soc. **127** (7), 1630-1635 (1980). DOI: https://doi.org/ 10.1149/1.2129965

[4] J.K. Doychak, The evolution and growth of Al_2O_3 scales on β-NiAl. Case Western Reserve University, Cleveland, OH, 1986.

[5] J. Jedlinski, S. Mrowec, The influence of implanted yttrium on the oxidation behaviour of β-NiAl. Mater. Sci. Eng. **87**, 281-287 (1987). DOI: https://doi.org/10.1016/0025-5416(87)90390-9

[6] B.A Pint, A. Jain, L.W, Hobbs, The Effect of Yttrium Ion Implantation on the High Temperature Oxidation Properties of NiAl. MRS Online Proceedings Library **213**, 981-986 (1990). DOI: https://doi.org/10.1557/PROC-213-981

[7] E. Schumann, The effect of Y-ion implantation on the oxidation of β-NiAl. Oxid. Met. **43**, 157-172 (1995). DOI: https://doi.org/10.1007/BF01046752

[8] I. Rommerskirchen, V. Kolarik, Oxidation of β-NiAl, undoped and doped with Ce, Y, Hf. Mater. Corros. **47**, 625-630 (1996). DOI: https://doi.org/10.1002/maco.19960471106

[9] J. Nesbitt, B.M. Gleeson, D. Sordelet, C.A. Barrett, Pt and Hf Additions to NiAl Bond Coats and their Effect on the Lifetime of Thermal Barrier Coatings. Mater. Sci. Forum **426-432**, 209-214 (2003). DOI: https://doi.org/10.1016/10.4028/www.scientific.net/msf.426-432.209

[10] B.A. Pint, The role of chemical composition on the oxidation performance of aluminide coatings. Surf. Coat. Technol. **188-189**, 71-78 (2004). DOI: https://doi.org/10.1016/j.surfcoat.2004.08.007

[11] J. Jedliński, High Temperature Oxidation and Oxidation-Induced Degradation of Alumina Formers. Mater. Sci. Forum, **595-598**, 995-1003 (2008). DOI: https://doi.org/10.4028/www.scientific.net/msf.595-598

[12] H. Svensson, M. Chistensen, P. Knutsson, G. Wahnström, K. Stiller, Influence of Pt on the metal–oxide interface during high temperature oxidation of NiAl bulk materials. Corros. Sci. **51**, 539-546 (2009). DOI: https://doi.org/10.1016/j.corsci.2008.12.016

[13] H.J. Choi, J. Jedliński, B. Yao, Y. Sohn, Transmission electron microscopy observations on the phase composition and microstructure of the oxidation scale grown on as-polished and yttrium-implanted β-NiAl. Surf. Coat. Techn. **205**, 1206-1210 (2010). DOI: https://doi.org/10.1016/j.surfcoat.2010.10.034

[14] J. Jedliński, J.L. Grosseau Poussard, G. Smoła, G. Bonnet, M. Nocuń, K. Kowalski, J. Dąbek, The effect of alloyed and/or implanted yttrium on the mechanism of the scale development on β-NiAl at 1100ºC. Mater. High Temp. **29** (2), 59-69 (2012). DOI: https://doi.org/10.3184/096034012x13349146318471

[15] D. Li, H. Guo, D. Wang, T. Zhang, S. Gong, H. Xu, Cyclic Oxidation of β-NiAl with Various Reactive Element Dopants at 1200ºC. Corros. Sci. **66**, 125-135 (2013). DOI: https://doi.org/ 10.1016/j.corsci.2012.09.010

[16] H. Guo, D. Wang, H. Peng, S. Gong, H. Xu, Effect of Sm, Gd, Yb,Sc and Nd as Reactive Elements on Oxidation Behaviour of β-NiAl at 1200ºC. Corros. Sci. **78**, 369-377 (2014). DOI: https://doi.org/10.1016/j.corsci.2013.10.021

[17] H.B. Guo, D.Q. Li, L. Zheng, S.K. Gong, H.B. Xu, Effect of co-doping of two reactive elements on alumina scale growth of *β*-NiAl at 1200°C. Corros. Sci. **88**, 197-208 (2014). DOI: https://doi.org/10.1016/j.corsci.2014.07.036

[18] R. Swadźba, Influence of hafnium on high temperature oxidation of NiAl and Ni_3Al alloys. Pr. Inst. Metal. Zelaza **70**, 19-29 (2018). DOI: https://doi.org/10.32730/imz.0137-9941.18.2.02

[19] Y. Zhu, W. Qian, F. Dai, Y. Ye, Y. Hua, J. Cai, Study of oxidation mechanisms of Ni-Al alloys with different phase structures at 1200°C. Mater. Today Communications. **35** [June], 106393 (2023). DOI: https://doi.org/ 10.1016/j.mtcomm.2023.106393

[20] D.P. Whittle, J. Stringer, Improvements in High Temperature Oxidation Resistance by Additions of Reactive Elements or Oxide Dispersions. Phil. Trans. Roy. Soc. Lond. **A295** [1413], 309-29 (1989). DOI: https://doi.org/10.1098/rsta.1980.0124

[21] J. Stringer, The reactive element effect in high-temperature corrosion, Mater. Sci. Eng. A, **120–121** [1], 129-137 (1989). DOI: https://doi.org/10.1016/0921-5093(89)90730-2

[22] J. Jedliński, The Influence of Reactive Elements on the High Temperature Oxidation Behavior of Alumina-Forming Materials. Solid State Phenomena **21-22**, 335-390 (1992). DOI: https://doi.org/10.4028/www.scientific.net/ssp.21-22.335

[23] J. Jedlinski, General aspects of the reactive element effect. Corros. Sci. **35**, 863-869 (1993). DOI: https://doi.org/10.1016/0010-938X(93)90302-W

[24] B.A. Pint, Progress in understanding the reactive element effect since the Whittle and Stringer literature review. In: Tortorelli PF, Wright IG, Hou PY, editors. Proc. John Stringer Symposium on High Temperature Corrosion. ASM International, Materials Park, OH, p. 9-19, 2003.

[25] B.A. Pint, Optimization of Reactive-Element Additions to Improve Oxidation Performance of Alumina-Forming Alloys. J. Am. Ceram. Soc. **86**, 686-695 (2003). DOI: https://doi.org/10.1111/j.1151-2916.2003.tb03358.x

[26] P.Y. Hou, The reactive elements effect - past, present and future. Mater. Sci. Forum **696**, 39-44 (2011). DOI: https://doi.org/10.4028/www.scientific.net/msf.696.39

[27] D. Naumenko, B.A. Pint, W.J. Quadakkers, Current Thoughts on Reactive Element Effects in Alumina-Forming Systems: In Memory of John Stringer. Oxid. Met. **86**, 1-43 (2016). DOI: https://doi.org/10.1007/s11085-016-9625-0

[28] B.A. Pint, Experimental observations in support of the dynamic-segregation theory to explain the reactive-element effect. Oxid. Met. **45**, 1-37 (1996). DOI: https://doi.org/10.1007/bf01046818

[29] A.H. Heuer, D.B. Hovis, J.J. Smialek, B. Gleeson, Alumina Scale Formation: A New Perspective. J. Am. Ceram. Soc. **94** (8), 2698-2698 (2011). DOI: https://doi.org/10.1111/j.1551-2916.2011.04777.x

[30] A.H. Heuer, T. Nakagawa, M.Z. Azar, D.B. Hovis, J.L. Smialek, B. Gleeson, N.D.M. Hine, H. Guhl, H.-S. Lee, P. Tangney, W.M.C. Foulkes, M.W. Finnis, On the growth of Al_2O_3 scales. Acta Mater. **61** (18), 6670-6683 (2013). DOI: https://doi.org/10.1016/j.actamat.2013.07.024

[31] V. Babic, C. Geers, I. Panas, Reactive Element Effects in High-Temperature Alloys Disentangled. Oxid. Met. **93**, 229-245 (2020). DOI: https://doi.org/10.1007/s11085-019-09946-6

[32] J. Doychak, J.L. Smialek, T.E. Mitchell, Transient oxidation of single-crystal beta-NiAl. Metall. Trans. **20A**, 499-518 (1989). DOI: https://doi.org/10.1007/BF02653930

[33] G.C. Rybicki, J.L. Smialek, Effect of the θ-α-Al_2O_3 transformation on the oxidation behavior of β-NiAl + Zr. Oxid. Met. **31**, 275-304 (1989). DOI: https://doi.org/10.1007/bf00846690

[34] M.W. Brumm, H.J. Grabke, The Oxidation Behaviour of NiAl- I. Phase Transformations in the Alumina Scale During Oxidation of NiAl and NiAl-Cr Alloys. Corrosion Science **33** (11), 1677-1690 (1992).
`DOI: https://doi.org/10.1016/0010-938x(92)90002-k

[35] J. Jedliński, Comments on the effect of reactive elements on the early stages of oxidation of alumina formers. Oxid. Met. **39**, 55-59 (1993). DOI: https://doi.org/ 10.1007/bf00666609

[36] J. Jedliński, M.J. Graham, G.I. Sproule, D.F. Mitchell, G. Borchardt, A. Bernasik, A Combined Approach : Isotopic Exposure / SIMS Analysis / SEM to Study the Early Stages of Oxidation of β-NiAl at 1473 K. Mater. Corros. **46**, 297 (1995).
DOI: https://doi.org/10.1002/maco.19950460505

[37] B.A. Pint, J.R. Martin, L.W. Hobbs, The oxidation mechanism of theta-Al_2O_3 scales. Solid, State Ionics **78**, 99-107 (1995).
DOI: https://doi.org/10.1016/0167-2738(95)00013-V

[38] D.M. Lipkin, H. Schaffer, F. Adar, D.R. Clarke, Lateral Growth Kinetics of α-Alumina Accompanying the Formation of a Protective Scale on (111) NiAl During Oxidation at 1100°C. Appl. Phys. Lett. **70** (19), 2550-52 (1997).
DOI: https://doi.org/10.1063/1.118917

[39] B.A. Pint, M. Treska, L.W. Hobbs, The Effect of Various Oxide Dispersions on the Phase Composition and Morphology of Al_2O_3 Scales Grown on β-NiAl. Oxid. Met. **47** (1/2), 1-20 (1997).
DOI: https://doi.org/10.1007/bf01682369

[40] J.C. Yang, E. Schumann, M. Ruehle, I. Levin, Transient oxidation of NiAl. Acta Mater. **46** (6), 2195-2201 (1998).
DOI: https://doi.org/10.1016/S1359-6454(97)00378-9

[41] V.K. Tolpygo, D.R. Clarke, Microstructural study of the theta-alpha transformation in alumina scales formed on nickel-aluminides. Mater. High Temp. **17** (1), 59-70 (2000).
DOI: https://doi.org/10.1179/mht.2000.011

[42] R. Bagwell, G. L. Messing, P. R. Howell, The formation of α-Al_2O_3 from θ-Al_2O_3: The relevance of a "critical size" and: Diffusional nucleation or "syncho-shear"? J. Mater. Sci. **36** (7), 1833-1841 (2001). DOI: https://doi.org/10.1023/A:1017545213590

[43] D. Oquab, D. Monceau, In-situ SEM study of cavity growth during high temperature oxidation of β-(Ni,Pd)Al. Scripta Mater. **44**, 2741-2746 (2001).
DOI: https://doi.org/ 10.1016/S1359-6462(01)00959-9

[44] D.D. Ragan, T. Mates, D.R. Clarke, Effect of Yttrium and Erbium Ions on Epitaxial Phase Transformations in Alumina. J. Am. Ceram. Soc. **86** (4), 541-45 (2003).
DOI: https://doi.org/10.1111/j.1151-2916.2003.tb03338.x

[45] J. Jedliński, Morphology and Microstructure of Oxide Scale Growing on High Temperature Alumina-Forming Materials. Ceramika, **80**, 893-897 (2003).

[46] E. Wallin, J.M. Andersson, V. Chirita, U. Helmersson, Effects of additives in alpha and theta-alumina: an ab initio study. J. Physics: Condensed Matter. **16**, 8971-8980 (2004).
DOI: https://doi.org/ 10.1088/0953-8984/16/49/012

[47] P.Y. Hou, A.P. Paulikas, B.W. Veal, Stress development and relaxation in Al_2O_3 during early stage oxidation of β-NiAl. Mater. High Temp. **22** (3/4), 535-543 (2005).
DOI: https://doi.org/ 10.3184/096034005782744146

[48] J.M. Alvarado-Orozco, R. Morales-Estrella, M.S. Boldrick, J.L. Ortiz-Merino, D.G. Konitzer, G. Trapaga-Martinez, J. Munoz-Saldana, First Stages of Oxidation of Pt-Modified Nickel Aluminide Bond Coat Systems at Low Oxygen Partial Pressure. Oxid. Met. **78**, 269-284 (2012).
DOI: https://doi.org/10.1007/s11085-012-9305-7

[49] G. Smoła, J. Jedliński, J.L. Grosseau-Poussard, B. Gleeson, G. Bonnet, M. Nocuń, K. Kowalski, A. Rakowska, On the phase composition changes during high temperature oxidation of Pt-modified β-NiAl at 1150°C. Mater. High Temp. **29** (2), 107-115 (2012).
DOI: https://doi.org/ 10.3184/096034012x13322363758903

[50] W. Zhao, Z. Li, B. Gleeson, A New Kinetics-Based Approach to Quantifying the Extent of Metastable-Stable Phase Transformation in Thermally-Grown Al_2O_3 Scales. Oxid. Met. **79**, 361-381 (2013).
DOI: https://doi.org/ 10.1007/s11085-012-9359-x

[51] X. Liang, X. Wang, Modeling of theta-alpha alumina lateral phase transformation with applications to oxidation kinetics of NiAl-based alloys. Materials and Design **112**, 519-529 (2016).
DOI: https://dx.doi.org/10.1016/j.matdes.2016.10.001

[52] J. Jedliński, R. Gołdyn, J.-L. Grosseau-Poussard, G. Bonnet, K. Kowalski, A. Bernasik, G. Smoła, J. Dąbek, M. Nocuń, Oxide phases and residual stresses in scales formed at early stages of oxidation of β-NiAl at 1473K and the effect of implanted yttrium. Mater. Corros. **68** (2), 235-248 (2017).
DOI: https://doi.org/10.1002/maco.201508774

[53] J. Jedlinski, J.L. Grosseau Poussard, J. Dabek, B. Gleeson, M. Nocuń, R. Gołdyn, The Effect of Pt Content on the Scale Development on β-NiAl at Very Early Oxidation Stages. Oxid. Met. **87** [3], 311-319 (2017).
DOI: https://doi.org/10.1007/s11085-017-9714-8

[54] Y. Huang, X. Peng, X-Q. Chen, The mechanism of θ- to α- Al_2O_3 phase transformation. J. Alloy. Compd. **863**, 158666 (2021).
DOI: https://doi.org/10.1016/ j.jallcom.2021.158666

[55] T.L. Barth, E.A. Marquis, Effects of Minor Alloying Elements on Alumina Transformation During the Transient Oxidation of β-NiAl. Oxid. Met. **95**, 293-309 (2021).
DOI: https://doi.org/10.1007/s11085-021-10024-z1 3

[56] Y.F. Yang, S.X. Ren, C.M. Deng, P. Ren, P.M. Zhang, R.L. Peng, Z.B. Bao, W. Li, Synergistic effect of Pt and Hf on the early-stage oxidation behaviour of NiAl coating at 1000°C. Corros. Commun. **5** (3), 49-61 (2022).
DOI: https://doi.org/10.1016/j.corcom.2021.11.007

[57] P. Burtin, J.P. Brunelle, M. Pijolat, M. Soustelle, Influence of surface area and additives on the thermal stability of transition alumina catalyst supports. I: Kinetic data. Appl. Catal. **34**, 225-238 (1987).
DOI: https://doi.org/10.1016/s0166-9834(00)82458-6

[58] P. Burtin, J.P. Brunelle, M. Pijolat, M. Soustelle, Influence of surface area and additives on the thermal stability of transition alumina catalyst supports. II: Kinetic Model and Interpretation. Appl. Catal. **34**, 239-254 (1987).
DOI: https://doi.org/10.1016/s0166-9834(00)82459-8

[59] C.K. Loong, J.W.R. Jr., M. Ozawa, Structural phase transformations of rare-earth modified transition alumina to corundum. J. Alloys Compd. **250**, 356-359 (1997).
DOI: https://doi.org/ 10.1016/S0925838896025509

[60] M. Schöneborn, J. Werner, T. Harmening, T. E. Weirich, Advances in the understanding of mesoporous transition aluminas: Unveiling the correlation between morphology and thermostability. J. Solid State Chem. **308**, 122906 (2022).
DOI: https://doi.org/10.1016/j.jssc.2022.122906

[61] S. Jang, D. Gun Oh, H. Kim, K. Hyun Kim, K. Khivantsev, L. Kovarik, J. Hun Kwak, Controlling the Phase Transformation of Alumina for Enhanced Stability and Catalytic Properties. Angew. Chem. Int. Ed. **136** (15), e202400270 (2024).
DOI: https://doi.org/10.1002/anie.202400270

[62] J. Jedlinski, Local and microstructure-related effects affecting the high temperature oxidation of alumina formers: A brief survey. Mater. High Temp. **12** (3-4), 485-495 (2005).
DOI: https://doi.org/10.1179/mht.2005.059

[63] J. Jedliński, Growth mechanism vs matter transport in thermally growing oxides on high temperature materials: A brief survey based on the case study of alumina formers. J. Defect and Diffusion Forum **289-292**, 385-395 (2009).
DOI: https://doi.org/10.4028/www.scientific.net/ddf.289-292.385

[64] X. Wang, A. Atkinson, L. Chirivi, J. R. Nicholls, Evolution of stress and morphology in thermal barrier coatings. Surf. Coat. Technol. **204**, 3851-3857 (2010).
DOI: https://doi.org/10.1016/j.surfcoat.2010.04.065